

First-order phase transition in the organic metal κ -(BETS)₂C(CN)₃

Bakhyt Zh. Narymbetov,^a Enric Canadell,^{*b} Tamaz Togonidze,^a Salavat S. Khasanov,^a Leokadiya V. Zorina,^a Rimma P. Shibaeva^{*a} and Hayao Kobayashi^c

^aInstitute of Solid State Physics, Russian Academy of Sciences, 142432 Chernogolovka, MD, Russia. E-mail: shibaeva@issp.ac.ru

^bInstitut de Ciència de Materials de Barcelona (CSIC), Campus de la U.A.B., E-08193 Bellaterra, Spain. E-mail: canadell@icmab.es

^cInstitute for Molecular Science, Okazaki, 444, Japan

Received 5th September 2000, Accepted 13th October 2000

First published as an Advance Article on the web 23rd November 2000

Evidence concerning the occurrence of a first-order phase transition around 260 K in the organic metal κ -(BETS)₂C(CN)₃ is reported and the effect of the transition on the crystal and electronic structure of the salt is discussed. Determination of the crystal structure at 50 K has shown that the main structural change brought about by the transition affects the anion sublattice. Although there are noticeable changes in the chalcogen...chalcogen short contacts of the donor lattice it is shown that the Fermi surface is left unaltered by both the first-order transition and the thermal contraction down to 50 K.

Recently, a new radical cation salt based on the bis(ethylenedithio)tetrathiafulvalene (BETS) donor, κ -(BETS)₂C(CN)₃, has been synthesised and the room temperature crystal and electronic structure, as well as the resistive properties, have been studied.^{1–2} This salt has a κ -type donor arrangement and metallic properties down to very low temperatures although it is not superconducting above 1.3 K. The lack of superconductivity might be related to the disorder in the BETS ethylenedithio groups and/or in the anion layers. For instance, an X-ray crystal structure of κ -(BETS)₂Cu[N(CN)₂]Br³ at 20 K showed that one of the ethylenedithio groups of BETS was still disordered even at this low temperature and this fact may be responsible for the failure to observe superconductivity in this salt, something which contrasts with the situation in the corresponding bis(ethylenedithio)tetrathiafulvalene (BEDT-TTF) salt.⁴ Thus, we thought it would be of interest to carry out a low temperature X-ray study which could shed light on this problem.

In addition, the observed Shubnikov–de Haas oscillations for this salt were not completely understood on the basis of the calculated Fermi surface. This was the reason for some concern because the Fermi surface was calculated on the basis of the room temperature crystal structure.¹ Thus, even if the main details of the surface are correct it could well be that differences between the room temperature and low temperature crystal structures could subtly affect its shape. In the present work we report new crystallographic data and resistivity measurements which make clear the existence of a first-order phase transition around 260 K in κ -(BETS)₂C(CN)₃. We also report a low temperature (50 K) crystal structure determination and discuss the effect of such a transition on the crystal and electronic structure of the salt.

Experimental

X-Ray structure determination†

X-Ray experimental data were collected at 50 K using the Weissenberg-type IP (image plate) system (DIP 320s, MAC

Science Co., Inc) equipped with a helium refrigerator.⁵ An absorption correction of intensities was not applied. The structure was solved by a direct method with the teXsan crystallographic software package⁶ and then refined by a full-matrix least-squares method in an anisotropic approximation (isotropic for H). The main crystal and experimental data for κ -(BETS)₂C(CN)₃ are presented in Table 1.

Band structure calculations

The tight-binding band structure calculations were based upon the effective one-electron Hamiltonian of the extended Hückel method.⁷ The off-diagonal matrix elements of the Hamiltonian were calculated according to the modified Wolfsberg–Helmholz formula.⁸ All valence electrons were explicitly taken into account in the calculations and the basis set consisted of double- ζ Slater-type orbitals for C, S and Se and single- ζ Slater-type orbitals for H. The exponents, contraction coefficients and

Table 1 Main crystal and refinement data for κ -(BETS)₂C(CN)₃ at 50 K^a

Chemical formula	C ₂₄ S ₈ H ₁₆ Se ₈ N ₃
Formula weight	1234.6
Crystal system	Monoclinic
Space group	<i>A2/a</i>
<i>Z</i>	4
<i>a</i> /Å	11.482(6)
<i>b</i> /Å	8.330(3)
<i>c</i> /Å	35.04(1)
β /°	94.87(4)
<i>V</i> /Å ³	3339(2)
<i>D</i> _{calc} /g cm ⁻³	24.55
μ /cm ⁻¹	92.8
Radiation, λ /Å	MoK α , 0.71069
<i>F</i> (000)	2324
2θ _{max}	59°
No. of reflections measured	6979
No. of independent reflections	4228
<i>R</i> _{int}	0.109
No. of observed reflections	2430 [<i>I</i> > 3 σ (<i>I</i>)]
No. of refined parameters	187
<i>R</i>	0.082

^aUnit cell parameters at room temperature: *a* = 11.583(3) Å, *b* = 8.475(1) Å, *c* = 35.086(5) Å, β = 91.10(2)°, *V* = 3444(1) Å³.¹

†CCDC reference number 1145/254. See <http://www.rsc.org/suppdata/jm/b0/b007174i/> for crystallographic files in .cif format.

atomic parameters for C, S, Se and H were taken from previous works.^{9–10}

Electrical resistivity measurements

The high quality crystal of κ -(BETS)₂C(CN)₃ used for the experiment was grown electrochemically as described in ref. 1. The interlayer (*i.e.* perpendicular to the highly conducting *ab* plane of the crystal) resistance was measured by the standard ac four-probe method at 330 Hz from room temperature down to 1.3 K.

Results and discussion

The variation of the unit cell parameters with temperature was measured from room temperature down to 30 K. The temperature dependence of the unit cell parameters is shown in Fig. 1. All the parameters exhibit clearly visible hysteresis, especially the parameter *a* and the angle β , as a consequence of a first-order phase transition occurring at around 260 K. Projections of the crystal structure of κ -(BETS)₂C(CN)₃ along the *b*-direction at room temperature and 50 K are shown in Figs. 2a and 2b, respectively. From the crystallographic viewpoint, the first-order phase transition is mainly characterised by changes in the anion layer but without a drastic modification of the basic crystal structure. Nevertheless, the changes in the anion layer affect the inner structure of the conducting BETS layers so that it is interesting to compare the structural details above and below the phase transition and its possible effect on the electronic structure.

The structure is characterised by BETS radical cation layers

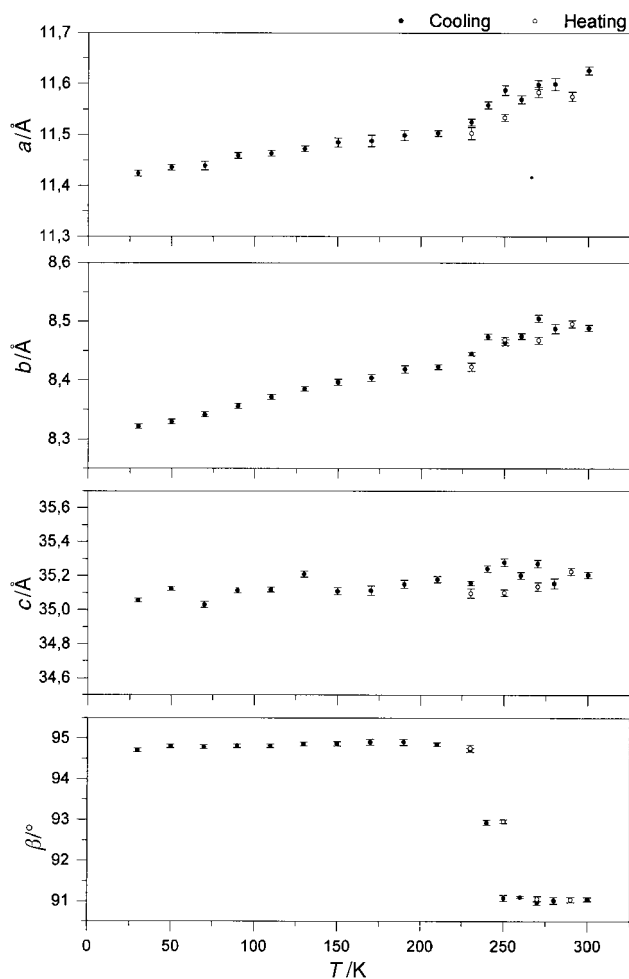


Fig. 1 Lattice constants as a function of temperature for the κ -(BETS)₂C(CN)₃ single crystals.

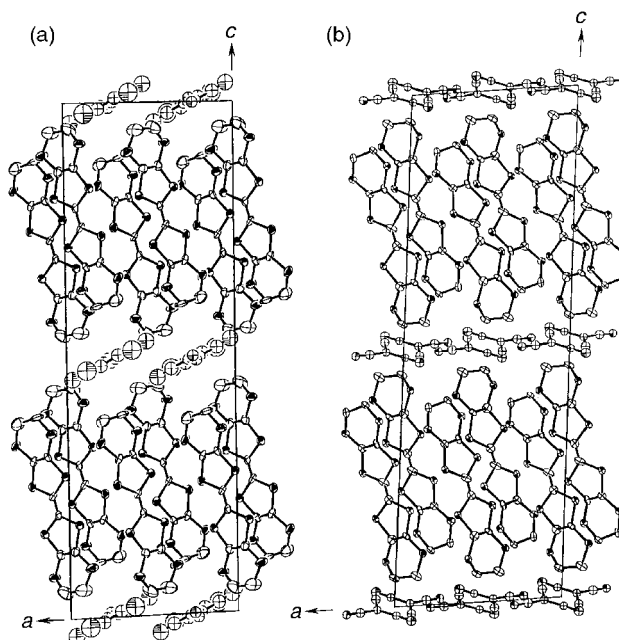


Fig. 2 Crystal structure of κ -(BETS)₂C(CN)₃ viewed along the *b*-axis: a) at 293 K, and b) at 50 K.

alternating with anion layers along the *c*-direction. The projection of the radical cation layer along the BETS molecular long axis is shown in Fig. 3a. The unit cell contains two BETS radical cation and two anion layers. The bond lengths and angles for the BETS radical cation at *T* = 50 K are listed in Table 2 (see Fig. 3b for the donor labelling). It is important to point out that whereas the ethylenedithio groups of BETS are disordered at room temperature, they are ordered at low temperature (see for instance the C7–C8 and C9–C10 bond lengths in Table 2).

As in all κ -phase salts, the radical cation layer is formed by dimers of the BETS donors oriented in a roughly orthogonal manner (the angle is about 80°). The intradimer distance

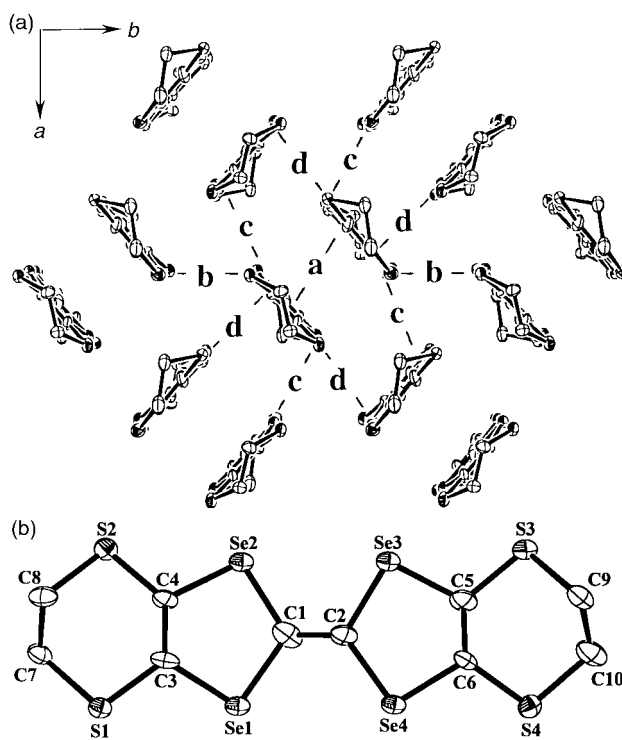


Fig. 3 a) Radical cation layer in κ -(BETS)₂C(CN)₃ viewed along the BETS molecular long axis, and b) labelling scheme for the BETS donor. The four different types of intermolecular interactions are shown in (a).

Table 2 Bond lengths $d/\text{\AA}$ and angles $\omega/^\circ$ for BETS at $T=50\text{ K}$

Bond	d	Angle	ω
Se1–C1	1.92(1)	C1Se1C3	92.9(6)
Se1–C3	1.91(1)	C1Se2C4	95.6(5)
Se2–C1	1.93(1)	C2Se3C5	93.6(6)
Se2–C4	1.90(1)	C2Se4C6	94.6(6)
Se3–C2	1.92(1)	C3S1C7	100.9(6)
Se3–C5	1.91(1)	C4S2C8	101.5(6)
Se4–C2	1.91(1)	C5S3C9	98.0(6)
Se4–C6	1.88(1)	C6S4C10	104.4(7)
S1–C3	1.80(1)	Se1C1Se2	112.8(7)
S1–C7	1.83(1)	Se1C1C2	125(1)
S2–C4	1.73(1)	Se2C1C2	122(1)
S2–C8	1.81(1)	Se3C2Se4	113.3(7)
S3–C5	1.78(1)	Se3C2C1	120(1)
S3–C9	1.77(1)	Se4C2C1	125(1)
S4–C6	1.77(1)	Se1C3S1	112.0(7)
S4–C10	1.81(1)	Se1C3C4	122(1)
C1–C2	1.26(2)	S1C3C4	125(1)
C3–C4	1.35(2)	Se2C4S2	112.9(7)
C5–C6	1.35(2)	Se2C4C3	116(1)
C7–C8	1.47(2)	S2C4C3	130(1)
C9–C10	1.56(2)	Se3C5S3	113.0(8)
		Se3C5C6	119(1)
		S3C5C6	127(1)
		Se4C6S4	113.7(7)
		Se4C6C5	119(1)
		S4C6C5	127(1)
		S1C7C8	114.0(9)
		S2C8C7	115(1)
		S3C9C10	112.0(9)
		S4C10C9	112(1)

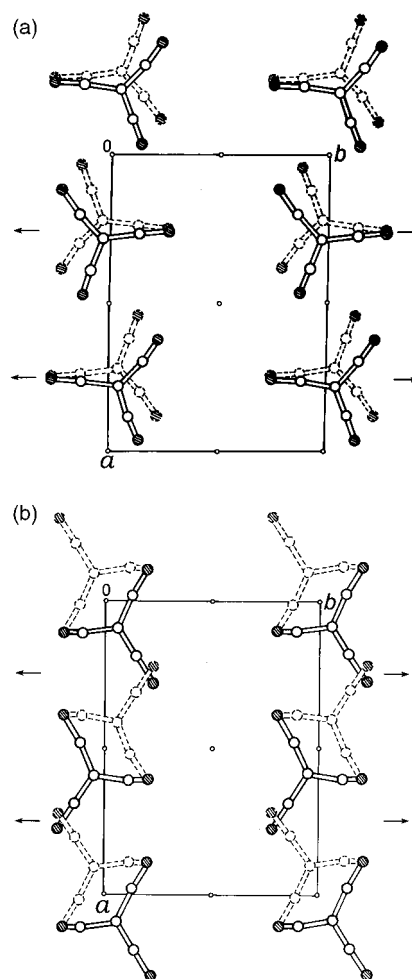
between the BETS molecular planes is 3.46 \AA (3.52 \AA at room temperature). The mode of intermolecular overlapping in the dimer has not changed at 50 K and it is of the so-called ring-over-bond type. However, there is some change in the molecular orientation: the angle which the average plane of BETS makes with the $[001]$ direction is 13.3° at low temperature but 9.8° at room temperature. In addition, the dihedral angle between the BETS and the anion $\text{C}(\text{CN})_3^-$ planes is quite different at low and room temperatures, *i.e.*, 55.4 and 84.4° , respectively. The radical cation layer contains a large number of short $\text{Se}\cdots\text{Se}$, $\text{Se}\cdots\text{S}$ and $\text{S}\cdots\text{S}$ contacts. Those shorter than the sum of the van der Waals radii, as well as the corresponding ones at room temperature, are listed in Table 3. It should be noted that not all of these contacts have been shortened when going from room temperature to 50 K .

Projections of the anion layer on the ab -plane at room temperature and 50 K are shown in Figs. 4a and 4b, respectively. A rather different picture of the anion layers

Table 3 $\text{Se}\cdots\text{Se}$ ($r \leq 3.90\text{ \AA}$), $\text{Se}\cdots\text{S}$ ($r \leq 3.80\text{ \AA}$) and $\text{S}\cdots\text{S}$ ($r \leq 3.70\text{ \AA}$) contacts between the BETS radical cations

Contact	$r/\text{\AA}$		BETS ^a	Interaction type ^b
	50 K	293 K		
Se1 \cdots Se2 (Se2 \cdots Se1)	3.851(1)	3.896(2)	$I-I_6$ ($I-I_3$)	c
Se1 \cdots Se3 (Se3 \cdots Se1)	3.822(1)	3.881(2)	$I-I_1$ ($I-I_1$)	a
Se1 \cdots S2 (S2 \cdots Se1)	3.621(3)	3.680(5)	$I-I_6$ ($I-I_3$)	c
Se2 \cdots Se4 (Se4 \cdots Se2)	3.751(1)	3.796(2)	$I-I_1$ ($I-I_1$)	a
Se3 \cdots Se4 (Se4 \cdots Se3)	3.669(1)	3.726(2)	$I-I_3$ ($I-I_6$)	c
Se3 \cdots S1 (S1 \cdots Se3)	3.581(3)	3.793(5)	$I-I_2$ ($I-I_4$)	d
Se3 \cdots S4 (S4 \cdots Se3)	—	3.761(5)	$I-I_3$ ($I-I_6$)	c
Se4 \cdots S1 (S1 \cdots Se4)	3.705(2)	—	$I-I_5$ ($I-I_5$)	b
Se4 \cdots S2 (S2 \cdots Se4)	3.616(3)	3.705(4)	$I-I_4$ ($I-I_2$)	d
S1 \cdots S2 (S2 \cdots S1)	3.694(4)	3.661(5)	$I-I_6$ ($I-I_3$)	c
S1 \cdots S4 (S4 \cdots S1)	3.614(4)	3.573(7)	$I-I_5$ ($I-I_5$)	b
S3 \cdots S4 (S4 \cdots S3)	3.537(4)	3.515(6)	$I-I_3$ ($I-I_6$)	c

^aSymmetry codes: I (x, y, z), I_1 ($-x, 0.5-y, 0.5-z$), I_2 ($0.5-x, y-0.5, 0.5-z$), I_3 ($x+0.5, 1-y, z$), I_4 ($0.5-x, y+0.5, 0.5-z$), I_5 ($-x, 1.5-y, 0.5-z$), I_6 ($x-0.5, 1-y, z$). ^bSee Fig. 3a for labelling.

**Fig. 4** Projection of the anion layer along the c -axis at: a) $T=293\text{ K}$ and, b) $T=50\text{ K}$.

can be seen in these figures. Although a disorder in the anion layer still exists at 50 K , the anion positions have changed with respect to those at room temperature. The $\text{C}(\text{CN})_3$ groups have rotated by approximately 20° around the $[001]$ direction. The $\text{C}(\text{CN})_3$ plane makes angles of 9.1 , 24.3 and 65.2° with the $[100]$, $[010]$ and $[001]$ directions at 50 K , whereas those at room temperature are 25.7 , 2.7 , 63.0° , respectively. Thus, the X-ray structural study of the single crystals of κ -(BETS) $_2\text{C}(\text{CN})_3$ below the first-order phase transition reveals that, as for $(\text{BEDO-TTF})_2\text{ReO}_4 \cdot \text{H}_2\text{O}$ (where BEDO-TTF is bis(ethylenedioxy)tetrathiafulvalene),¹¹ the transition is mainly connected with changes in the anion layer: a reorientation of the $\text{C}(\text{CN})_3^-$ anions at 260 K causes the decrease of the a , b , c -parameters and the jump of the monoclinic angle, which increases noticeably (Fig. 1).

It should be noted that during the low temperature X-ray study some intermediate state between 240 and 250 K has been observed. Additional reflections mainly of diffuse character appeared in this temperature interval. The experimental data give us ground to suppose that the intermediate state is disordered, having a primitive cell. Probably, the low and high temperature phases coexist here and the positions of the $\text{C}(\text{CN})_3$ anions are mixed.

Finally, it is worth pointing out that the κ -(BETS) $_2\text{C}(\text{CN})_3$ radical cation salt is not isostructural with the corresponding BEDT-TTF salt, $(\text{BEDT-TTF})_2\text{C}(\text{CN})_3$,¹² which exhibits a metal-insulator phase transition at $\sim 180\text{ K}$. In that case the phase transition was found to be of the Peierls type. The band electronic structure predicted a doubling of the b -axis as a consequence of the Peierls distortion, which was confirmed by

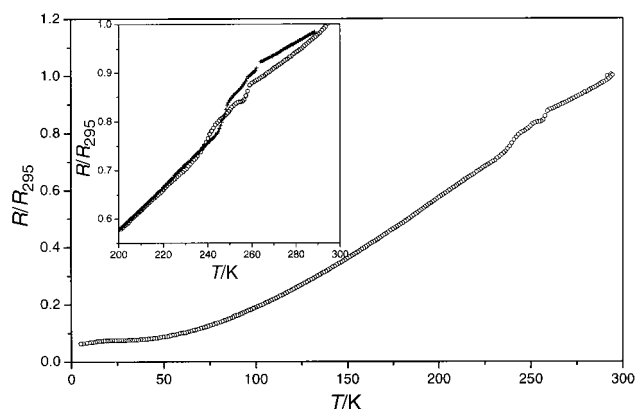


Fig. 5 Temperature dependence of the resistivity of κ -(BETS)₂C(CN)₃. In the insert “circles” refer to the cool-down process and “crosses” to the warm-up process (The room temperature resistivity is $\sim 45.5 \Omega \text{ cm}$).

taking X-ray photographs of (BEDT-TTF)₂C(CN)₃ as a function of temperature.

The temperature dependence of the resistivity of κ -(BETS)₂C(CN)₃ is shown in Fig. 5 (the cooling (warming) velocity was of approximately 1.6 K min^{-1} and the room temperature resistivity is $\sim 45.5 \Omega \text{ cm}$). Some anomalous behaviour is clearly visible in the temperature interval 240–260 K, the same temperature range in which some intermediate state was observed during the X-ray study.

In order to consider how the above mentioned changes in the donor layer influence the band structure and Fermi surface, we have calculated the $\beta_{\text{HOMO-HOMO}}$ intermolecular interaction energies,¹³ which are a measure of the interaction between two HOMOs in adjacent sites of the layer, on the basis of both the room temperature and the 50 K crystal structures (see Table 4). There are four different types of donor···donor intermolecular interactions in the donor layer (see Fig. 3a). Two of them implicate donor molecules which are almost parallel to each other (either within a dimer (**a**) or between two donors of different dimers (**b**)) and two implicate donor molecules which are almost orthogonally oriented (**c** and **d**). According to the values in Table 4, the effect of the transition (and thermal contraction) on the electronic structure is weak. Not only are the changes in the HOMO–HOMO intermolecular interactions quite modest, but also the relative change of the two strong interactions (**a** and **b**) is weak (*i.e.*, only 10.8 and 5.1%, respectively). In addition, the changes of the **c** and **d** interactions, although relatively large, partially compensate each other.

These changes are not difficult to understand when the variation in the chalcogen···chalcogen short contacts, the directionality of the orbitals leading to the HOMO–HOMO overlap, and the larger overlap when a Se atom is implicated in a short intermolecular contact, are taken into account. For instance, all chalcogen···chalcogen contacts of interaction **d** decrease at low temperature, some of them by as much as 0.2 \AA , leading to an increase in the strength of the interaction. In contrast, for interaction **c** some of the short chalcogen···chalcogen contacts decrease but others increase, the final outcome

Table 4 Comparison of the absolute values of the $\beta_{\text{HOMO-HOMO}}$ intermolecular interaction energies (eV) calculated for the 50 K and room temperature structures of κ -(BETS)₂C(CN)₃

Interaction type ^a	50 K	293 K
a	0.7053	0.6366
b	0.3461	0.3294
c	0.0764	0.1051
d	0.1713	0.1205

^aSee Fig. 3a for labelling.

being a decrease of the interaction strength because of orbital orientation reasons. For interaction **b** the changes also go in opposite directions, leading to a small change in the strength of the interaction, whereas four of the strong Se···Se short contacts of interaction **a** decrease at low temperature, leading to the largest change in the intermolecular interactions. However, interaction **a** does not influence the dispersion of the partially filled pair of bands of the κ -phases.

Thus, the modest changes of interactions **b**, **c** and **d**, as well as their partial compensation, suggest that no major changes on the electronic structure of κ -(BETS)₂C(CN)₃ must be expected to result from the first-order phase transition (and the thermal contraction). This is in complete agreement with our tight binding calculations using the 50 K crystal structure. Both the Fermi surface and band structure are practically identical with those we previously reported for the room temperature crystal structure¹ and thus will not be reported here again. For instance, using the 50 K crystal structure, the calculated area of the lens-like closed portion of the Fermi surface and the density of states at the Fermi level are 21.9% and 1.37 electrons *per* eV and *per* donor molecule, respectively. These values are practically indistinguishable from those calculated for the room temperature crystal structure (21.9% and 1.38, respectively). This explains why the first-order transition only slightly affects the resistivity of the salt.

The excellent agreement between the calculated and experimentally determined cross-sectional area (22%) of the lens-like closed orbit of the Fermi surface (that the magnetic breakdown cross-sectional area must be 100% is imposed by the stoichiometry of the salt) fully supports the previously calculated two-dimensional Fermi surface for κ -(BETS)₂C(CN)₃. Thus, the origin of the reported additional low frequency oscillations of the magnetoresistance^{1,2} still remains elusive. The present study suggests that it is necessary to know in detail the three-dimensional Fermi surface of this salt in order to progress along this line. Further experimental and theoretical studies are clearly in order.

Conclusion

As a result of the present study it may be concluded that there is a first-order phase transition in κ -(BETS)₂C(CN)₃ at 260 K mainly involving the anion layer. However, this does not mean that the changes are not (at least partially) transmitted to the donor layer. Indeed, several Se···S, Se···Se and S···S short contacts change noticeably although these changes leave the Fermi surface practically unaltered and thus, the transition only weakly affects the resistivity of the salt. Interestingly, the terminal ethylenedithio groups of BETS are ordered at low temperature, strongly suggesting that it is the disorder in the anion sublattice which is at the origin for the absence of superconductivity in this κ -type salt. Let us note that structural phase transitions have also been observed in other radical cation salts with κ -type conducting layers like κ -(BEDT-TTF)₄PtCl₆·C₆H₅CN,^{14–16} κ -(BEDT-TTF)₂[CuN(CN)₂]Br¹⁷ and (BEDT-TTF)₄(Et₄N)M(CN)₆·3H₂O, where M = Co, Fe.^{18,19} In the present case, some intermediate disordered state was observed in the temperature range 240–250 K. The existence of such a kind of state has been inferred from both the X-ray diffraction study and some peculiarity of the resistivity curves (Fig. 5). However, the nature of the intermediate phase could not be estimated by the traditional X-ray structure analysis.

Acknowledgments

This work was supported by the NWO program, RFBR (Russian Foundation for Basic Research) grant 99-02-16119, the Russian National Program ‘Physics of Quantum wave

processes', DGES (Spain) Project PB96-0859 and Generalitat de Catalunya (1999 SGR 207). We thank M. Kartsovnik, N. D. Kushch and E. B. Yagubskii for their interest in this work.

References

- 1 B. Zh. Narymbetov, N. D. Kushch, L. V. Zorina, S. S. Khasanov, R. P. Shibaeva, T. G. Togonidze, A. E. Kovalev, M. V. Kartsovnik, L. I. Buravov, E. B. Yagubskii, E. Canadell, A. Kobayashi and H. Kobayashi, *Eur. Phys. J. B*, 1998, **5**, 179.
- 2 T. G. Togonidze, A. E. Kovalev, M. V. Kartsovnik, E. Canadell, N. D. Kushch and E. B. Yagubskii, *Synth. Met.*, 1999, **103**, 1969.
- 3 T. Burgin, T. Miebach, J. C. Huffman, L. K. Montgomery, J. A. Paradis, C. Rovira, M.-H. Whangbo, S. N. Magonov, S. I. Khan, C. E. Strouse, D. L. Overmyer and J. E. Schirber, *J. Mater. Chem.*, 1995, **5**, 1659.
- 4 A. M. Kini, U. Geiser, H. H. Wang, K. D. Carlson, J. M. Williams, W. K. Kwok, K. G. Vandervoort, J. E. Thompson, D. L. Stupka, D. Jung and M.-H. Whangbo, *Inorg. Chem.*, 1990, **29**, 2555.
- 5 A. Kobayashi, T. Naito and H. Kobayashi, *Phys. Rev. B*, 1995, **51**, 3198.
- 6 TeXsan: Crystal Structure Analysis Package, Molecular Structure Corp., The Woodlands, USA, 1985 & 1992.
- 7 M.-H. Whangbo and R. Hoffmann, *J. Am. Chem. Soc.*, 1978, **100**, 6093.
- 8 J. Ammeter, H.-B. Bürgi, J. Thibeault and R. Hoffmann, *J. Am. Chem. Soc.*, 1978, **100**, 3686.
- 9 A. Pénicaud, K. Boubekour, P. Batail, E. Canadell, P. Auban-Senzier and D. Jérôme, *J. Am. Chem. Soc.*, 1993, **115**, 4101.
- 10 A. Pénicaud, P. Batail, C. Coulon, E. Canadell and C. Perrin, *Chem. Mater.*, 1990, **2**, 123.
- 11 S. S. Khasanov, B. Zh. Narymbetov, L. V. Zorina, L. P. Rozenberg, R. P. Shibaeva, N. D. Kushch, E. B. Yagubskii, R. Rousseau and E. Canadell, *Eur. Phys. J. B*, 1998, **1**, 419.
- 12 M. A. Beno, H. H. Wang, L. Soderholm, K. D. Carlson, L. N. Hall, L. Nunez, H. Rummens, B. Anderson, J. A. Schlueter, J. M. Williams, M.-H. Whangbo and M. Evain, *Inorg. Chem.*, 1989, **28**, 150.
- 13 (a) M.-H. Whangbo, J. M. Williams, P. C. W. Leung, M. A. Beno, T. J. Emge and H. H. Wang, *Inorg. Chem.*, 1985, **24**, 3500; (b) Since overlap is explicitly included in the extended Hückel calculations, these interaction energies (β) should not be confused with the conventional transfer integrals (t). Although the two quantities are obviously related and have the same physical meaning, the absolute values of β are somewhat larger than those of t .
- 14 A. A. Galimzyanov, A. A. Ignat'ev, N. D. Kushch, V. N. Laukhin, M. K. Makova, V. A. Merzhanov, L. P. Rozenberg, R. P. Shibaeva and E. B. Yagubskii, *Synth. Met.*, 1989, **33**, 81.
- 15 V. E. Korotkov, V. N. Molchanov and R. P. Shibaeva, *Sov. Phys. Crystallogr. (Engl. Transl.)*, 1992, **37**, 776.
- 16 M.-L. Doublet, E. Canadell and R. P. Shibaeva, *J. Phys. I*, 1994, **4**, 1479.
- 17 Y. Nogami, J.-P. Pouget, H. Ito, T. Ishiguro and G. Saito, *Solid State Commun.*, 1994, **89**, 113.
- 18 P. Le Magueres, L. Ouahab, N. Conan, C. J. Gomez-Garcia, P. Delhaes, J. Even and M. Bertault, *Solid State Commun.*, 1996, **97**, 27.
- 19 P. Le Magueres, L. Ouahab, P. Briard, J. Even, M. Bertault, L. Toupet, J. Ramos, C. J. Gomez-Garcia, P. Delhaes and T. Mallah, *Synth. Met.*, 1997, **86**, 1859.